Available online at www.sciencedirect.com
ScienceDirect
Surface & Coatings Technology 201 (2007) 7115–7121
SURFACE & COATINGS TECHNOLOGY
www.elsevier.com/locate/surfcoat

Oscillating composition of Fe–W alloy thin films grown by magnetron co-sputtering

P. Plantin [a], A.-L. Thomann [a,*], P. Brault [a], P.-O. Renault [b], S. Laaroussi [c], P. Goudeau [b], B. Boubeker [c], T. Sauvage [d]

[a] Groupe de Recherches sur l'Energétique des Milieux ionisés, UMR 6606 CNRS-Université d'Orléans, Polytech'Orléans BP6744, 45067 Orléans Cedex2, France
[b] Laboratoire de Métallurgie Physique, UMR 6630 CNRS-Université de Poitiers, SP2MI BP 30172, 86962 Futuroscope Cedex, France
[c] Laboratoire de Contrôle et de Caractérisation des Matériaux, Université Hassan II, Km9 Route d'El Jadida, Casablanca, Marocco
[d] Centre d'Etudes et de Recherches par Irradiation, UPR 33 CNRS, 3A avenue de la recherche scientifique, 45071 Orléans Cedex 2, France

Received 6 September 2006; accepted in revised form 8 January 2007
Available online 16 January 2007

Abstract

Fe–W alloy coatings were deposited by D.C. magnetron co-sputtering at room temperature. Initial results from Rutherford Backscattering Spectroscopy (RBS) have evidenced in-depth variation in the film chemical composition, which oscillates between $Fe_{0.19}W_{0.81}$ and $Fe_{0.29}W_{0.71}$. The deposits are multilayer systems composed of elementary alloy layers, with a thickness of the order of several tens of nanometers. In the present work, we study the influence of two deposition parameters on this particular in-depth composition modulation: substrate rotation rate and deposition time. The thickness of the elementary layers depends on the rotation rate of the substrate holder, as expected from what is reported in the literature on pure nanolayer synthesis in planar magnetron geometry. Surprisingly, the composition oscillations disappear for the longest deposition times (above 3 min). Alloy films (with or without composition oscillations) are found to exhibit the same morphology and crystalline structure as pure W. It is evidenced that Fe atoms are located in substitution in the W atomic structure and that an amorphous phase of alloy is also formed.

PACS: 81.15.Cd; 68.55.Jk; 68.55.Nq
Keywords: Magnetron sputtering; Alloy; Iron; Tungsten

1. Introduction

In the cathode-ray tube displays used for televisions, an iron (Fe) mask (200 μm thick foil drilled with 200×400 μm holes) located between the electron beam and the screen is used to define the elementary color grid. Under the electron beam action, this foil is heated and may be stretched out of shape, inducing a loss in the image quality. In order to avoid damage cause to the mask by heating, coatings have been developed to improve the mechanical and thermal properties of iron foils under electron beam bombardment. To achieve this aim, they should not be affected by the part of the energy that is absorbed, i.e. a temperature gradient should be avoided. Moreover, coatings have to exhibit high electron backscattering and good emissivity coefficients in order to dissipate a significant part of the incoming energy. Tungsten (W) is chosen because of its good refractory properties and its high electron backscattering coefficient (β=0.48) [1].

In a recent work [2], thin Fe films were deposited on a 300 nm W layer and postoxidized to form Fe_3O_4 (magnetite), which has a good IR emissivity coefficient. Fortunately, it has been shown that the post-oxidation industrial process used, did not perturb the W underlayer. Indeed WO_3 formation has to be avoided because its electron backscattering coefficient is lower than that of pure W. Moreover, WO_3 has poor adhesion to the Fe substrate. The deposition conditions of both Fe and W layers have been defined in order to ensure good adhesion to the

* Corresponding author. GREMI Polytech'Orléans, 14 rue d'Isssoudun, BP 6744, 45067 Orléans cedex2, France. Tel.: +33 238494870; fax: +33 238417154.
E-mail address: anne-lise.thomann@univ-orleans.fr (A.-L. Thomann).

0257-8972/$ - see front matter © 2007 Elsevier B.V. All rights reserved.
doi:10.1016/j.surfcoat.2007.01.014

substrate and efficient superficial Fe layer oxidation. A bilayer system Fe_3O_4 (≈300 nm)/W (≈300 nm)/Fe foil has shown promising properties for the desired application.

In a second step, we decided to synthesize thin films of Fe–W alloys, in order to take advantage of both W and Fe properties, and then to compare their potential mechanical and thermal properties with bilayer thin films. Moreover, the Fe–W system is worth being studied, since it is known for other numerous interesting properties [3]. From Monte Carlo simulations [4], it has been shown that the dissipation of the energy deposited by the electron beam in the material is mainly located in the protective coating (as required) when the alloy composition is close to $Fe_{0.3}$ $W_{0.7}$. Consequently, the study was focused on this composition. On primary synthesized alloy films, in-depth composition has been found to oscillate between two stoichiometries. To our knowledge, this behavior has not been reported before in the literature for metallic binary systems. However, several papers report on the synthesis of pure metallic bilayers by magnetron co-sputtering [5–7]. This phenomenon, i.e. obtaining pure layers during simultaneous sputtering of targets, is observed when the deposition is performed at very low substrate rotation rate. In these studies, the substrate surface is successively exposed to one then another magnetron. To obtain an alloy (usually metastable), further annealing process is necessary [8]. The synthesis of thicker pure layers requires alternate sputtering of each magnetron [5,6].

In the present work, we study the formation conditions and the nature (stoichiometry, crystalline structure etc.) of the composition oscillations that we have evidenced on Fe–W alloy films obtained by magnetron co-sputtering. Since the substrate rotation rate appears to induce the formation of separate pure layers in particular co-sputtering geometries, we have chosen to vary this parameter as well as the deposition time. RBS was used to estimate the film thickness and composition. Scanning Electron Microscopy (SEM) was carried out to study the surface morphology. From X-ray diffraction (XRD), the crystalline structure was investigated.

2. Experimental setup

The magnetron sputtering system (APRIM Vide) used in this work is equipped with three independent magnetron targets, 30° tilted relative to the substrate surface. It has been widely described elsewhere [9]. A schematic of the geometrical arrangement is drawn in Fig. 1.

Targets were pure W (99.999%) and Fe (99.999%) disks with a diameter of 10 cm. The target to substrate distance was kept at 9 cm, ensuring overlapping of the neutral atom fluxes reaching the substrate surface. The base pressure in the deposition chamber was maintained below 10^{-4} Pa by a turbo molecular pump (ATP900, ALCATEL). The Fe substrates (foils of 200 μm thickness) were transferred into the sputtering vacuum chamber after being cleaned in an acetone ultrasonic bath and ethanol rinsed. The grounded substrate was rotated to ensure in-plane homogeneous film composition and thickness uniformity. The rotation rate was varied in the range 0.8 to

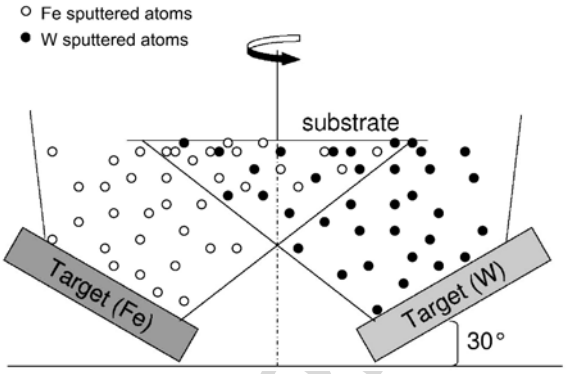

Fig. 1. Schematic drawing of the targets and substrate arrangements.

6 rotations/min (rpm). The substrate was not cooled during deposition. For binary Fe–W alloy synthesis, both magnetrons were switched on together. Target powers were kept constant (500 W for W and 300 W for Fe) in order to obtain the desired stoichiometry: $Fe_{0.3}W_{0.7}$, taking into account the element sputtering yields. The argon deposition pressure was 2.8×10^{-1} Pa. In these conditions, the Fe and W deposition rates are: 30 nm/min and 40 nm/min, respectively. The deposition times ranged from 1 min. 30 s to 5 min. In addition to Fe foils (10×10 cm), Si (100) wafers (several cm^2) were used as substrates. They were pasted at the center of an Fe foil fixed on the substrate holder which is designed for 10×10 cm substrates. For Fe substrates, analyses were realized on samples cut in the middle of the foil (about 1 cm^2).

RBS measurements were carried out on a Van de Graff accelerator, using 2 MeV $^4He^+$ ion (α particles) beam. The beam spot size on the samples was about 2×2 mm. Au/Si, C, Ni/Si and Si samples were used as references for energy calibration of the spectra. The silicon barrier detector (about 13 keV energy resolution) was placed 9 cm away from the sample. The α particles reach the detector with a backscattering angle of 165°. The RBS spectra were simulated using SIMNRA code [10]. The results of this analysis give for each layer the total number of the present atoms by cm^2, which can be converted into an equivalent thickness with an assumption on the density (at/cm^3). The crystalline structure of the layers was studied by XRD. X-ray diffraction measurements were carried out using a commercial Bruker D5005 diffractometer equipped with a forward monochromator, using CuKá radiation. Two kinds of XRD measurements were performed in θ–2θ mode and in Ω–2θ (with Ω fixed at 3°). Surface morphology was observed by SEM (Hitachi: S-4500, CME-Université d'Orléans, Orléans, France). Deposits on Si substrate are dedicated to grazing incidence XRD analysis for which a flat surface is required. RBS and SEM characterization of alloy films synthesized (in the same deposition conditions) on Fe foils or Si wafers has shown that the chemical composition, thickness and surface morphology do not depend on the substrate nature. This allows us to deduce the crystalline structure of the alloys from the deposits performed on Si wafers.

3. Experimental results

3.1. RBS results

Fe–W alloy was deposited on Fe substrate. Typical experimental and simulated RBS spectra are given in Fig. 2. Oscillations are clearly visible on the W and Fe contributions. They are fitted by an alternation of individual layers with alloy composition $Fe_{0.19}W_{0.81}$ or $Fe_{0.29}W_{0.71}$. The atomic percentages are mean values calculated from 3 or 4 samples synthesized in the same deposition conditions. The corresponding uncertainties are of the order of ±2% and mainly depend on the deposition parameter reproducibility. The uncertainty coming from the spectrum fit is very low, less than 0.5%. Even if low (10–20%), this composition modulation is unambiguously detected by RBS and reproducible. Since the oscillating behavior of the composition is better resolved on the W peak, it will be presented in the following.

The RBS spectra in Fig. 3 display the composition of the films depending on the deposition time (Fig. 3(a)) and substrate rotation rate (Fig. 3(b)). Oscillations are clearly visible, especially at short deposition times and low rotation rates. At a given rotation rate (Fig. 2a), whatever the time, as long as the oscillations are detectable, the composition and thickness of the elementary layers do not change. The only feature which depends on the deposition time is the total film thickness; i.e. the number of elementary layers. For example, at 3 rpm, the fit of the RBS spectra gives 10, 14, 20 elementary layers (10 nm thick) for 1 min. 30 s, 2 min and 3 min deposition times, respectively. This corresponds to 100 nm, 140 nm and 200 nm total thicknesses. Note that the thicknesses are estimated from RBS assuming an alloy film density close to that pure W. This hypothesis is in agreement with SEM observations which evidence that the alloy micro-structure is the same as the W layer one (see Section 3.2). In Fig. 3(a) (3 rpm) after 3 min., the oscillations are no longer well defined, which was not expected. This point will be discussed below.

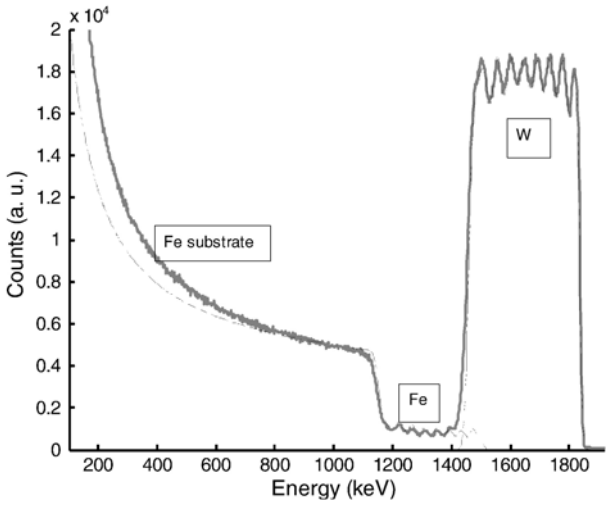

Fig. 2. Typical experimental and simulated RBS spectra. They were obtained for 1.5 rpm rotation rate, 5 min deposition time deposit.

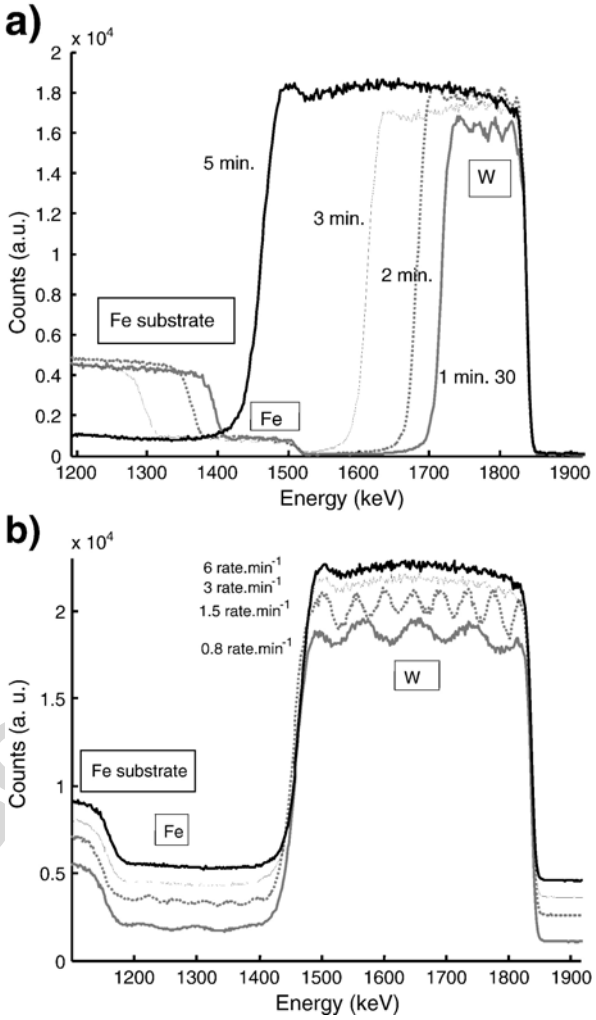

Fig. 3. RBS experimental spectra of alloy samples synthesized: a) at various deposition times and for a substrate rotation rate of 3 rpm, b) at various substrate rotation rates for 5 min deposition time.

On the RBS spectra in Fig. 3(b) and in Table 1, it can be seen that when the rotation rate increases, the thickness of the individual layers decreases. However, the composition of these elementary layers is the same whatever the rotation rate. Above 3 rpm, oscillations disappear because layers become too thin to be detected by RBS. RBS depth resolution can be estimated to 12 nm for Fe and 10 nm for W at the surface. For higher substrate rotation rates, elementary layers can no longer be defined and the composition becomes homogeneous over all the film.

Table 1
Variation of the individual layer thickness (calculated from RBS results) versus the substrate deposition rate

Rotation rate (rpm)	Individual layer thickness (nm)
0.8	36
1.5	19
3	10
6	–

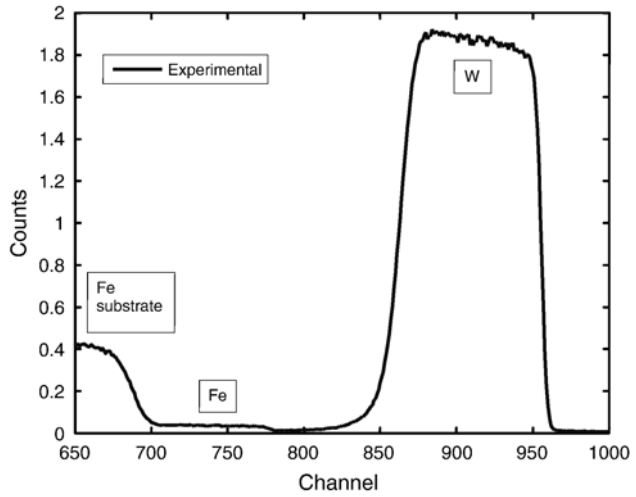

Fig. 4. RBS experimental spectrum of alloy sample prepared at 1 min 30 sec deposition time without substrate rotation.

The oscillatory behavior of the composition does not exist when the deposition is performed without substrate rotation as can be seen in Fig. 4. The chemical composition at the center of the foil is homogeneous over the whole thickness (W: 85 at.% and Fe: 15 at.%).

3.2. SEM results

In Fig. 5, the SEM picture presents the typical morphology of the alloy films, which is independent of the rotation rate and the deposition time. This morphology resembles flakes oriented perpendicular or parallel to the substrate surface. This is in good agreement with what is observed on pure W layers synthesized in our experiment. Wang et al. [9] have shown that the morphology of W deposits on Cu also have the same morphology. SEM observations of alloy film cross sections evidence the columnar structure usually observed in magnetron sputtering films [11–13], which has also been found on pure W films [6] (see Fig. 6).

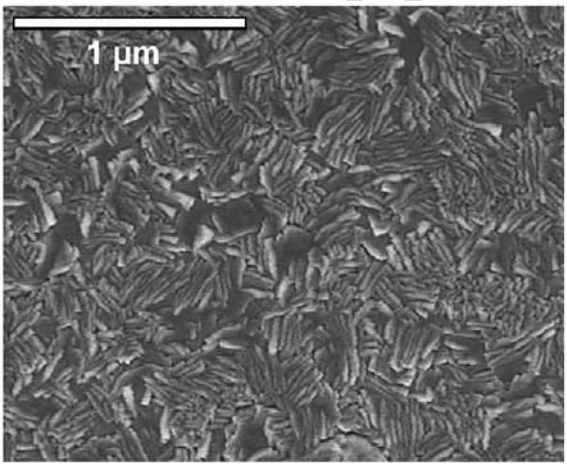

Fig. 5. SEM picture (×50,000, 5 kV) of a sample prepared at 5 min and 3 rpm deposition condition.

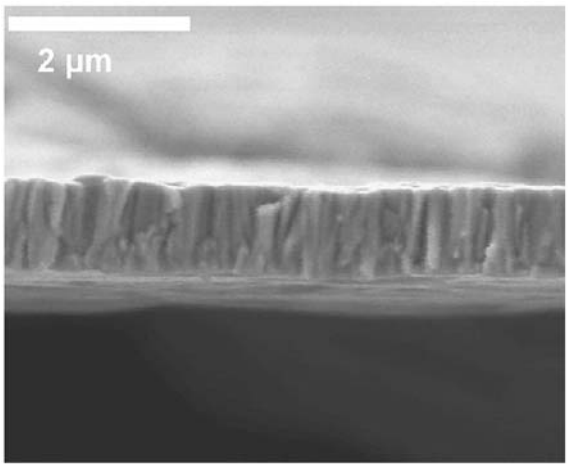

Fig. 6. Typical SEM cross section (×25,000, 5 kV) of a pure W layer deposited on Fe foil.

3.3. XRD analysis

Fig. 7(a) shows the XRD θ–2θ scans and Fig. 7(b) the XRD diffractogram performed for a fixed incident angle of Ω=3° and 2θ scans. The main synthesized phase has a body centered cubic (BCC) crystalline structure close to α-W (JCPDS powder diffraction file number 88-2339). The diffraction peaks are shifted to larger 2θ values compared to pure bulk W. The crystalline part of the film is thus composed of W solid solution with a lattice parameter smaller than pure W bcc (a=0.31648 nm). Neither pure Fe nor Fe intermetallic compounds (Fe_2W and Fe_7W_6) [14,15] published by the

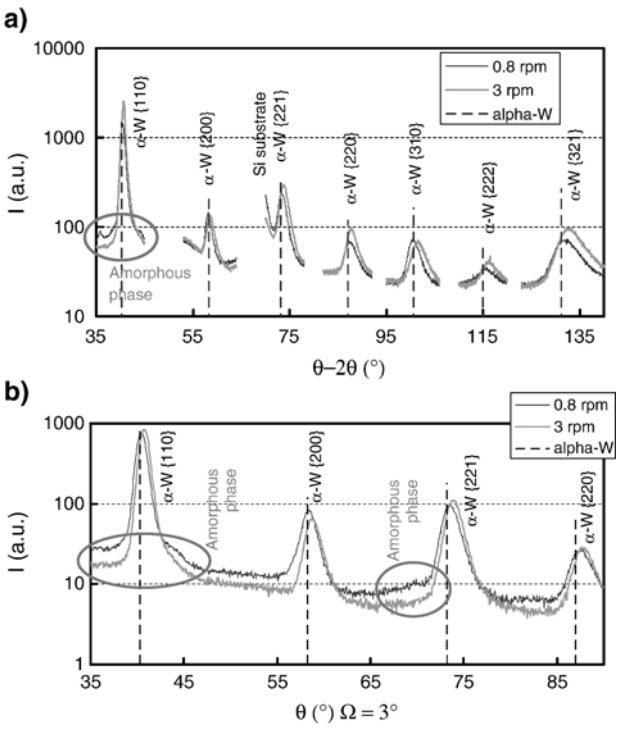

Fig. 7. XRD diffractograms of samples synthesized at various rotation rates and for 5 min deposition time: a) (θ–2θ) graph; b) θ graph at Ω=3°.

International Center of Diffraction Data (ICDD) were detected. This is true whatever the deposition time and rotation rate. For the 0.8 rpm sample, the two small shoulders around the (110) peak of the W solid solution can be attributed to the presence of an amorphous phase such as the ones observed by Huang et al. [14]. As can be seen on the XRD patterns, each {*hkl*} plane is visible, indicating that there is no strong texture.

4. Discussion

A periodic oscillating chemical composition is found at low substrate rotation rate and short deposition time in Fe–W alloy films. The deposits are composed of alternating elementary nanolayers with $Fe_{0.19}W_{0.81}$ or $Fe_{0.29}W_{0.71}$ composition. The observation of inhomogeneous in-depth composition during co-deposition has been reported in the literature, but only when the experimental arrangement is such that the substrate surface passes alternately above the magnetron targets. For example, pure nanolayers of Al and Ti are obtained by Ramos et al. [5] by co-sputtering of planar magnetron targets at a low substrate rotation rate. Our configuration is also different from that used by Ludwig et al. [16] to synthesize multilayers of wedge films. In this case, two alloyed targets in planar geometry are used. The substrate is moved from one side into and out of the sputtering plasmas. In the present work, both magnetrons being tilted 30° relative to the surface of the substrate, an overlapping of the W and Fe atom fluxes exists everywhere at the substrate surface. However, at low rotation rates, the substrate side exposed to one of the targets is enriched in the corresponding component (see Fig. 1). The thickness period directly depends on the rotation rate. No oscillations are detected when deposition occurs without rotation of the substrate, clearly proving that the oscillatory behavior of the composition is due to this parameter. In contrast, the composition of the alloy layers is not related to the substrate rotation rate, as expected. Indeed, the percentage of one element versus the other above each magnetron only depends on the delivered powers that we decided to keep constant in all experiments to reach the desired composition: $Fe_{0.3}W_{0.7}$.

On SEM pictures, the alloy film morphology is found to be similar to that of W which is consistent with the fact that W is the main component of the alloy.

XRD results show that the Fe–W crystalline part of the thin films is composed of a W(Fe) solid solution in which Fe atoms are thought to substitute the W ones. Even though the films are composed of two alloys, the composition of the two phases is so close that a mean lattice parameter of BCC structure can be extrapolated from the peak positions. This gives a lattice parameter of the W solid solution smaller than the atomic diameter of the W atom (0.137 nm). This result has also been obtained by many authors [17–21], on Fe–W alloy films synthesized by mechanical alloying or plasma sputtering. On the XRD diffractograms of Lu et al. [16] for $Fe_x W_{(1-x)}$ alloys, BCC phase peaks are observable for composition $x \leq 30$ at.% and $x \geq 80$ at.%, whereas an amorphous phase is observed for 40 at.% $< x <$ 70 at.%. In our case, x (19–29 at.%) lies near the frontier between both domains. Thus the coexistence of a crystalline and an amorphous phase seems possible in this intermediate composition range. According to Lu et al. [17], the Fe–W alloy amorphous phase is characterized by an intense broad peak close to the (110) position and a smaller one close to the (211) one. Shoulders are observable on our diffractograms (see Fig. 7(b)), around these peaks, confirming the presence of an amorphous phase. It is not possible at this time to determine whether crystalline and amorphous phases lie well separated in different layers. However, taking into account Lu et al's work, it is more likely that the crystalline W(Fe) solid solution mainly appears in $Fe_{0.19}W_{0.81}$ layers, whereas the amorphous structure is stabilized in the $Fe_{0.29}W_{0.71}$ ones instead.

Using Vegard's law [22], with the lattice parameters obtained, the solid solubility of Fe in W can be calculated and is 4% for the 0.8 rpm sample and (8–9)% for the 3 rpm sample. It should be noted that residual stresses cannot be the reason for the peak shift in the Fe–W thin films. For instance, a high compressive residual stress state of 1 GPa in W would only induce a shift of the (110) peak of 0.06° towards lower 2θ angles, which is considerably lower than the measured values ($\Delta\theta = 0.16$–$0.46°$, see Table 2).

It is known that Fe and W have very limited mutual solid solubilities of only a few percent (<2.6 mol%) under equilibrium conditions [18,19] and intermetallic compounds including Fe_2W and Fe_7W_6 exist in this system [14,15]. In our experiment, none of these compounds are formed, and the percentages of Fe incorporated in the W structure are quite large. They are above the values obtained by mechanical alloying (5 at.%), a technique that is known to extend the solubility limits of binary systems [18]. This is not so surprising however, since it is known that in magnetron deposition processes, film synthesis conditions are far from equilibrium, and that the composition domains of metallic solid solution may be significantly enlarged [23].

Thus, XRD results indicate that among the 19–29 at.% of Fe detected by RBS, a small part (from 4% to 9%) forms a crystalline solid solution with W, whereas the remainder lies in an Fe-rich alloy amorphous phase. Even if the mean composition of elementary layers is the same whatever the substrate rotation rate, it is interesting to note that the amount of Fe diluted in the crystalline phase slightly increases with this parameter. This can be explained by kinetics. At low rotation rates, the substrate stays longer over each magnetron (thicker elementary layers). Above the iron target, a large number of Fe

Table 2
Measurements of the position and the FWHM of the α-W(Fe) phase peaks

	Pure W (ICDD)		Sample 1 Rotation rate : 0.8 rpm			Sample 3 Rotation rate : 3 rpm		
{*hkl*}	2θ	*a*	2θ	FWHM	*a*	2θ	FWHM	*a*
110	40.26	3.1654	40.42	1.04	3.1534	40.72	0.97	3.1311
200	58.28	3.1638	58.34	1.48	3.1608	58.73	1.94	3.1417
211	73.2	3.1646	73.49	1.74	3.1539	73.84	1.65	3.1411
220	87.02	3.1646	87.44	2.2	3.1524	87.77	2.14	3.1430

Deduction of the corresponding lattice parameter.

atoms are inserted inside the W structure but they have time to diffuse away, at the grain boundaries for example, where they stabilize the amorphous phase (Fe-rich structure). The system tends towards the equilibrium, thus lowering the Fe percentage in the crystalline W(Fe) solid solution. On the contrary, at high rotation rates, Fe atoms trapped in the tungsten structure during deposition close to the iron target have not time to move out, and high Fe atomic percentages are obtained.

The broad Full Width at Half Maximum (FWHM) of the diffraction peaks is characteristic of either a small grain size (Coherent Diffracting Domain-CDD—in the nanometer range) and/or a high content of microstrains. The classical XRD analysis of microstrains and CDD evaluations such as Williamson–Hall or, the simpler Scherrer's formula for grain size estimation, can not be used in this study, since the Fe–W films being formed of elementary nanolayers of slightly different compositions, broadening of the XRD peaks occurs. Schematically the films are composed of two BCC phases with two different lattice parameters. This difference is slight, but measured diffraction peaks result from the overlapping of two contributions. If the FWHM is due to such a cause, it should increase with the 2θ angles, which is shown in Table 2.

After a long deposition time, oscillations are no more observed even at the surface. This is quite surprising. It is known that the in-depth RBS resolution decreases with the thickness because of the energy straggling effect of the α particles going across the sample [24]. However, at the surface, oscillations should still be detected. In the literature, Friesen et al. [25] report that annealing (about 400 °C) of thin bilayer of Ti–BN obtained by co-deposition induces alloy formation. So we can surmise that after several minutes deposition time, the temperature of the substrate, which is not cooled, increases. Using thermal paper at the substrate bottom, the temperature was found above 100 °C (maximum temperature that this kind of paper can reach) after 5 min deposition time. It could be thought that this kind of annealing, occurring during the deposition process, may cause a mixing of the thin elementary alloy layers and the formation of a single alloy, i.e. the obtaining of a homogenous composition over the whole thickness. To check this hypothesis, an ex-situ annealing of a sample, on which oscillations were clearly visible, was performed in argon atmosphere at 500 °C for 1 h. After this treatment, oscillations were still detected by RBS. This result rules out our first hypothesis. Another cause for the disappearance of the oscillations on RBS spectra may be the surface roughness which is usually found to increase with the deposition time [26]. However, Atomic Force Microscopy measurements performed on deposits (Si substrates) have evidenced a low roughness mean square: RMS ≤ 10 nm. This value does not vary in the range of deposition time used in this work. Moreover, simulations of RBS spectra by SIMNRA, taking into account such a roughness, shows that oscillations are detectable. Thus, the disappearance of the composition oscillating behavior at long deposition times remains unexplained for the moment.

5. Conclusions

Fe–W alloy film synthesis by co-sputtering of tilted magnetron targets has been studied. Two deposition parameters have been varied: substrate rotation rate and deposition time. The rotation rate is found to be responsible for the alloy composition oscillating behavior and determines the elementary nanolayer thickness. The absence of oscillations at long deposition times remains unclear and does not come from heating or roughening during deposition.

Phase structure and morphology of the alloy, irrespective of the presence of composition oscillations, are the same as pure α-W. In the magnetron deposition process, the Fe–W alloy is formed in nonequilibrium conditions; a crystalline Fe–W solid solution has been synthesized with a content of Fe in W higher than the solid solubility under equilibrium conditions. The obtained compositions lie between 4 and 9 at.%. However, the content of Fe in the α-W structure is much smaller than the global Fe content measured by RBS in the film (19–29 at.%). Thus, Fe also seems to be present in an Fe-rich alloy amorphous phase, which is detected on XRD diffractograms. The physical and mechanical properties of these alloys are under study.

Acknowledgements

P. Plantin would like to thank CRT Plasma-Laser for a research fellowship. Le Ministère de la Recherche, the European Union, la Région Centre, la Communauté de l'Agglomération du Drouais, le Conseil Général de l'Eure et Loir are acknowledged for financial support. Y. Tessier is acknowledged for technical help in performing RBS analysis. G. Coudrat is acknowledged for valuable technical help.

References

[1] M. Dapor, Phys. Rev., B 46 (2) (1992) 618.
[2] P. Plantin, A.-L. Thomann, P. Brault, B. Dumax, J. Mathias, T. Sauvage, A. Pineau, Surf. Coat. Technol. 200 (1–4) (2005) 408.
[3] A. Piatkowska, J. Jagielski, G. Gawlik, W. Matz, E. Richter, M. Mozetic, A. Zalar, Wear 254 (2003) 1037.
[4] CASINO software: http://www.gel.usherbrooke.ca/casino/What.htm, D. Drouin, A.R. Couture.
[5] A. Ramos, M. Vieira, Surf. Coat. Technol. 200 (1–4) (2005) 326.
[6] J. Hampshire, P.J. Kelly, D.G. Teer, Thin Solid Films 447–448 (2004) 392.
[7] A.F. Jankowski, P.L. Perry, Thin Solid Films 193/194 (1990) 799.
[8] M. Cekada, P. Panjan, D. Juric, J. Dolinsek, A. Zalar, Thin Solid Films 459 (2004) 267.
[9] C. Wang, P. Brault, C. Zaepffel, J. Thiault, A. Pineau, T. Sauvage, J. Phys. D: Appl. Phys. 36 (3) (2003) 2709.
[10] M. Mayer, A simulation program for the analysis of NRA, RBS and ERDA, in technical reports IPP9/113, Max-Planck-Institut fur Plasma Physik, Garching, 1997.
[11] A. Dirks, R. Wolters, A. De Veirman, Thin Solid Film 208 (2) (1992) 181.
[12] T. Vink, W. Walrave, J. Daams, A. Dirks, J. Appl. Phys. 74 (2) (1993) 988.
[13] Y. Shen, Y. Mai, Q. Zhang, D. McKenzie, W. McFall, W. McBride, J. Appl. Phys. 87 (1) (2000) 177.
[14] X.S. Huang, T. Mashimo, J. Alloys Compd. 296 (2000) 183.
[15] Y. Ustinovshkov, I. Dapegina, J. Mater. Sci. 39 (2004) 6233.
[16] A. Ludwig, Appl. Surf. Sci. 223 (2004) 78.
[17] M. Lu, C.L. Chien, J. Appl. Phys. 67 (9) (1990) 5787.
[18] E. Jartych, J.K. Zurawicz, D. Oleszak, M. Pekala, J. Magn. Magn. Mater. 218 (2000) 247.

[19] T.D. Shen, K.Y. Wang, M.X. Quan, J.T. Wang, J. Appl. Phys. 71 (4) (1991) 1967.
[20] X.S. Huang, T. Mashimo, J. Mater. Process. Technol. 85 (1999) 135.
[21] M.S. Boldrick, E. Yang, C.N.J. Wagner, J. Non-Cryst. Solids 150 (1992) 478.
[22] L. Vegard, Z. Phys. 5 (1921) 17.
[23] A. Billard, F. Perry, Les Techniques de l'Ingénieur «Pulvérisation cathodique magnétron» M1 654 (2005) 1.
[24] W. Bolse, Mater. Sci. Eng., R 12 (2) (1994) 53.
[25] T. Friesen, J. Haupt, W. Gissler, A. Barna, P. Barna, Surf. Coat. Technol. 48 (1991) 169.
[26] P. Meakin, Phys. Rep. 235 (1993) 189.